Radial Turbocompressor Chord Length Approximation for the Reynold's Number Calculation

Yannick Lattner* and Marius Geller

Department of Mechanical Engineering, University of Applied Sciences and Arts Dortmund

*Corresponding author: yannick.lattner@fh-dortmund.de

Abstract

We present an approximation model for the chord length of radial turbocompressors. The model enables the calculation of a compressor's chord Reynold's number during the machine design process. The chord Reynold's number is shown to be the most accurate representation of the fluid dynamic properties inside the radial turbocompressor's impeller. It — however — requires the computation of the chord length, which is only available after defining the final impeller geometry. The method presenting in this paper only employs the compressors principal dimensions to approximate the chord length. The chord is modelled using a Bézier spline and quarter ellipse. This enables the earlier use of the chord Reynold's number during the machine design process of radial turbocompressors.

Keywords: **Radial turbocompressors, Reynold's number, Turbomachinery, Design methods**

1   Introduction

The Reynold's number is an important property of centrifugal compressors. It is used to compare flow conditions for different machines, estimate properties like the efficiency and scale compressors (e.g, [1–3]).

Nomenclature

Superscripts and Subscripts			
c	Chord	b	Impeller width in m
Hub	Hub's spanwise location	c	Chord length in m
m	Mean spanwise location	c	Velocity in $\mathrm{m\,s^{-1}}$
$Shroud$	Shroud's spanwise location	D	Diameter in m
Symbols		L	Characteristic length in m
β	Relative blade angle in °	n	Rotational velocity in $1/\mathrm{s}$
μ	Dynamic viscosity in $\mathrm{Pa\,s}$	r	Radius in m
ν	Kinematic viscosity in $\mathrm{m^2\,s^{-1}}$	Re	Reynold's number
ν	Length ratio	u	Circumferential velocity in $\mathrm{m\,s^{-1}}$
ρ	Density in $\mathrm{kg\,m^{-3}}$	w	Relative velocity in $\mathrm{m\,s^{-1}}$
θ	Circumferential blade angle in °	z	Cartesian z-coordiante

The Reynold's number is a non-dimensional number. It is used to describe and compare flows for many applications. In general, it measures the ratio of the fluid's inertial forces and viscous forces. The Reynold's number is defined as [4]:

$$Re = \frac{cL}{\nu} = \frac{\rho c L}{\mu} \tag{1}$$

The characteristic length L has to be defined for each application. The Reynold's number for pipes is normally computed using an equivalent hydraulic diameter. To compare the flow over a plate, the length is usually used.

For many fluids flow conditions, a constant mean velocity c is observed. Turbomachinery — however — feature changing velocity values, as they transfer energy from or to the fluid. Multiple definitions of the Reynold's number have been proposed for radial turbocompressors. They are based on different analogies (Flow through a pipe; flow over a plate) and are thus employing different characteristic lengths and velocity values.

These different Reynold's number definitions are discussed in Section 2. The advantages of the chord Reynold's number are presented, and its definition is given. The actual chord length of a radial turbocompressor's impeller is not available during the machine design process. An approximation based only on machine design parameters is introduced in Section 3. This approximation is used to compute the chord Reynold's number in Section 4. Finally, a conclusion is given in Section 5

2 Reynold's number definitions for radial turbocompressors

Literature for radial turbocompressors often employ the circumference Reynold's number based on the impeller's outer diameter D_2 and the impeller tip speed u_2 [5–7]:

$$Re_u = \frac{u_2 \cdot D_2}{\nu} \tag{2}$$

A different approach describes the flow in the impeller as equivalent to a flow though a pipe [1]. Here, the impeller's exit width b_2 is used as equivalent hydraulic diameter:

$$Re_u = \frac{u_2 \cdot b_2}{\nu} \tag{3}$$

This approach has — however — limited usages. In [1], it is used for compressors, which have narrow impeller outlets ($b_2/D_2 < 0.03$). For those impellers, the boundary layers at hub and shroud can merge.

For general uses, both definitions feature weaknesses. They both use general properties of the impeller [8]. The impeller diameter D_2 being one. The circumferential velocity may be expressed by the impeller diameter D_2 and the impeller speed n:

$$u_2 = D_2 \pi n \tag{4}$$

The impeller exit width is usually defined by the ratio with the impeller diameter:

$$\nu_{b_2} = \frac{b_2}{D_2} \tag{5}$$

This ratio will be determined during the compressor's design process and, thus, be determined by the overall machine design.

The chord Reynold's number is a more realistic representation of the radial turbocompressor's internal flow field. It is computed using the relative velocity of the impeller inflow w_1 and the actual length of the flow path along the impeller blade, the chord length c [8]:

$$Re_c = \frac{w_1 \cdot c}{\nu} \tag{6}$$

3 Chord Length Approximation

To compute the chord Reynold's number Re_c (Equation 6), the chord length c has to be computed. The chord length is determined by the impeller's shape, which is defined when the compressor is created using Computer-aided design (CAD). At this stage, the compressor's machine design properties are usually fully defined. Thus, the chord Reynold's number may not be used during the machine design process. This prevents the use of Reynold's number-based design methods and correlations.

To enable an earlier application of the chord Reynold's number, the chord is modeled using the impeller's principal dimensions. The chord's coordinates are computed using two paths:

1. The chord's projection onto the $r - \theta$ plane (in z-direction) and

2. the chord's projection onto the $r - z$ plane (in θ-direction).

The projection in the direction of the axis of rotation ($r - \theta$-plane) is represented by a

Bézier spline. The chord's projection onto the $r - z$ plane equals the meridional path of the selected spanwise location. A quarter ellipse represents it.

In this study, the mean spanwise location is used for the definition of the chord Reynold's number. Thus, the mean inlet diameter D_{1_m} is computed. This diameter divides the inlet region in two equal areas:

$$D_{1_m} = \left[\frac{1}{2} \left(D_{1_{Shroud}}^2 + D_{1_{Hub}}^2 \right) \right]^{\frac{1}{2}} \tag{7}$$

The chord's coordinates at the impeller inflow (C1) and outflow (C2) are thus known. Using the r, θ, z-coordinates:

$$\mathrm{C1} = \begin{bmatrix} D_{1_m}/2 \\ \theta_1 = 0° \\ 0\,\mathrm{m} \end{bmatrix}, \quad \mathrm{C2} = \begin{bmatrix} D_2/2 \\ \theta_2 \\ D_2 \left(\nu_L - \nu_{b_2} \right) \end{bmatrix} \tag{8}$$

In Cartesian coordinates (x, y, z), the points are expressed as follows:

$$\mathrm{C1} = \begin{bmatrix} 0\,\mathrm{m} \\ D_{1_m}/2 \\ 0\,\mathrm{m} \end{bmatrix}, \quad \mathrm{C2} = \begin{bmatrix} D_2/2 \sin\theta_2 \\ D_2/2 \cos\theta_2 \\ D_2 \left(\nu_L - \nu_{b_2} \right) \end{bmatrix} \tag{9}$$

The chord's projection onto the r, θ plane is now approximated using a Bézier spline. As the $r - \theta$-plane is co-planar to the $r - z$ plane, the spline is defined in Cartesian coordinates. The spline connects the points c_1 and c_2. It is defined by four control points (`CP1`...`CP4`). The coordinates of the first and fourth control point of the spline are defined in accordance to Equation 9:

$$\begin{bmatrix} x_{\mathrm{CP1}} \\ y_{\mathrm{CP1}} \end{bmatrix} = \begin{bmatrix} 0\,\mathrm{m} \\ D_{1_m}/2 \end{bmatrix} \tag{10}$$

$$\begin{bmatrix} x_{\mathrm{CP4}} \\ y_{\mathrm{CP4}} \end{bmatrix} = \begin{bmatrix} D_2/2 \sin\theta_2 \\ D_2/2 \cos\theta_2 \end{bmatrix} \tag{11}$$

To ensure a stable spline definition, the respective Euclidean distance from `CP1` to `CP2` and from `CP3` to `CP4` is set to $(D_2 - D_{1_m})/4$. At the leading edge, the relative blade angle β_1 is not acting in the x, y plane. Thus, the second control point's location can be chosen freely. It is placed at the same Cartesian y-coordinate as `CP1`. Its x-coordinate is chosen to be equal to $(D_2 - D_{1_m})/4$.

$$\begin{bmatrix} x_{\mathrm{CP2}} \\ y_{\mathrm{CP2}} \end{bmatrix} = \begin{bmatrix} (D_2 - D_{1_m}) \frac{1}{4} \\ D_{1_m} \end{bmatrix} \tag{12}$$

To obtain the location of the third control point, an auxiliary point `AP3` is placed on the line connecting the origin and `CP4` at the predefined distance to `CP4`. The distance is again

equal to $(D_2 - D_{1_m})/4$. The coordinates of the auxiliary point AP3 are thus:

$$\begin{bmatrix} x_{\text{AP3}} \\ y_{\text{AP3}} \end{bmatrix} = \frac{1}{2} \left(D_2 - \frac{D_2 - D_{1_m}}{2} \right) \begin{bmatrix} \sin \theta_2 \\ \cos \theta_2 \end{bmatrix} \tag{13}$$

To obtain the trailing edge's relative blade angle β_2, which does act in the x, y-plane, the auxiliary point is rotated around the fourth control point. The rotation matrix $R(\beta_2)$ specifies the rotation of AP3 around CP4.

$$R(\beta_2) = \begin{bmatrix} \cos \beta_2 + \frac{\pi}{2} & -\sin \beta_2 + \frac{\pi}{2} \\ \sin \beta_2 + \frac{\pi}{2} & \cos \beta_2 + \frac{\pi}{2} \end{bmatrix} \tag{14}$$

Control point 3 is now calculated as:

$$\begin{bmatrix} x_{\text{CP3}} \\ y_{\text{CP3}} \end{bmatrix} = \begin{bmatrix} x_{\text{CP4}} \\ y_{\text{CP4}} \end{bmatrix} + R(\beta_2) \begin{bmatrix} x_{\text{AP4}} - x_{\text{AP3}} \\ y_{\text{AP4}} - y_{\text{AP3}} \end{bmatrix} \tag{15}$$

The spline's control points are thus defined. The coordinates of the spline are computed using a resolution of $n = 100$ points. Figure 1 shows the final Bézier spline and its control points.
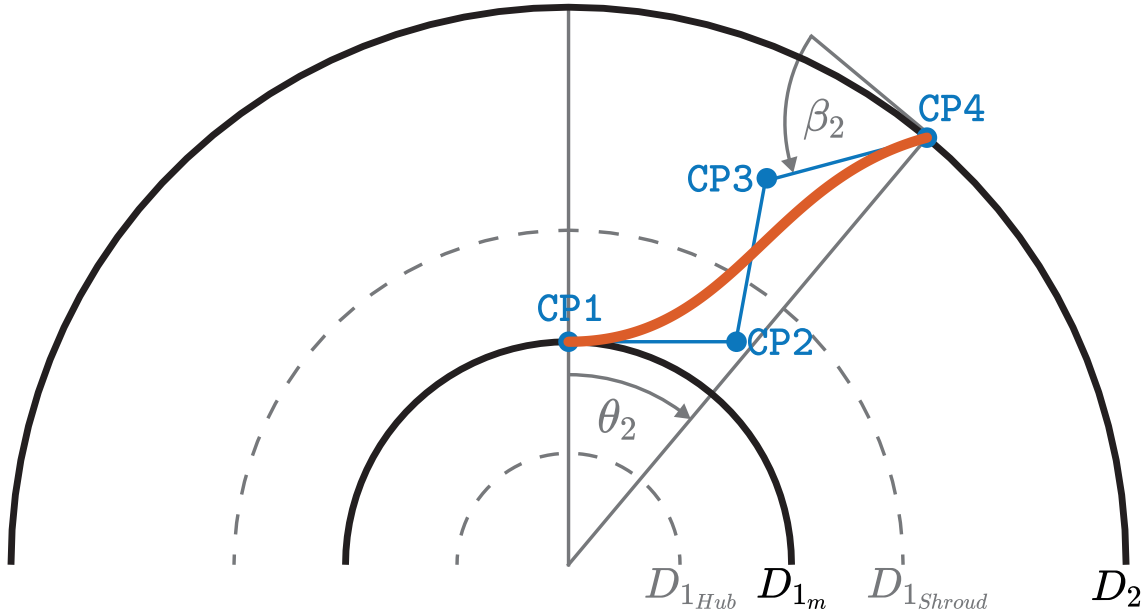
Figure 1: Bézier spline, defined to approximate the x, y components of the chord.

Having defined the chord's projection onto the x, y-plane, the third dimension is defined using the chord's projection onto the r, z plane. This is done by defining a quarter ellipse. The r, z coordinates of the ellipse's origin E0, the start point E1 and the end point E2 are

defined using Equation 8 and Equation 9:

$$\mathrm{E0} = \begin{bmatrix} D_2 \\ 0\,\mathrm{m} \end{bmatrix}, \quad \mathrm{E1} = \begin{bmatrix} D_{1_m} \\ 0\,\mathrm{m} \end{bmatrix}, \quad \mathrm{E2} = \begin{bmatrix} D_2 \\ \left(\nu_L - \frac{\nu_{b_2}}{2}\right) D_2 \end{bmatrix} \tag{16}$$

Thus, the ellipse's radii are:

$$\begin{bmatrix} r_1 \\ r_2 \end{bmatrix} = \mathrm{E2} - \mathrm{E1} = \begin{bmatrix} D_2 - D_{1_m} \\ \left(\nu_L - \frac{\nu_{b_2}}{2}\right) D_2 - 0\,\mathrm{m} \end{bmatrix} \tag{17}$$

The ellipse's coordinates are using the ellipse's equation [9] and an angle ϕ:

$$\begin{bmatrix} r_{\mathrm{E}} \\ z_{\mathrm{E}} \end{bmatrix} = \mathrm{E0} + \begin{bmatrix} r_1 sin(\phi) \\ r_2 cos(\phi) \end{bmatrix} \quad \text{with} \quad \phi = [{}^{3\pi}/2, \pi] \tag{18}$$

The ellipse is calculated for $1,000$ points.

To compute the chord's coordinates, the spline and the quarter ellipse must be made compatible. As the spline is defined in x, y-coordinates and the ellipse in r, z-coordinates, the data has to be adjusted. For each spline point, the radius r is computed.

$$r_{\mathrm{Spline}} = \sqrt{x^2 + y^2} \tag{19}$$

The data point of the ellipse with $r_{\mathrm{Spline}} = r_{\mathrm{E}}$ is identified for each of the spline's data points. The corresponding z-coordinate of this point is added to the spline's x, y-coordinate. The chord is now described completely using x, y, z-coordinates. Together with the spline and the ellipse, the combined chord path is shown in the three-dimensional plot in Figure 2.

Finally, the chord length is obtained by computing the sum of all neighboring entries' Euclidean distances.

$$c = \sum_{i=1}^{n-1} \sqrt{(x_{i+1} - x_i)^2 + (y_{i+1} - y_i)^2 + (z_{i+1} - z_i)^2} \tag{20}$$

4 Chord Reynold's number

As the chord length c is now available, the fluid mechanic properties w_1 and ν have to be obtained. As the chord Reynold's number is computed for the mean inlet diameter D_{1_m}, the velocity at this diameter has to be used for the calculation of the Reynold's number:

$$u_{1_m} = \pi n D_{1_m}; \tag{21a}$$

$$c_{1_m} = c_{1_{Hub}} + \frac{(c_{1_{Shroud}} - c_{1_{Hub}})(D_{1_m} - D_{1_{Hub}})}{D_{1_{Shroud}} - D_{1_{Hub}}} \tag{21b}$$

$$w_{1_m} = \left(c_{1_m}^2 + u_{1_m}^2\right)^{\frac{1}{2}} \tag{21c}$$
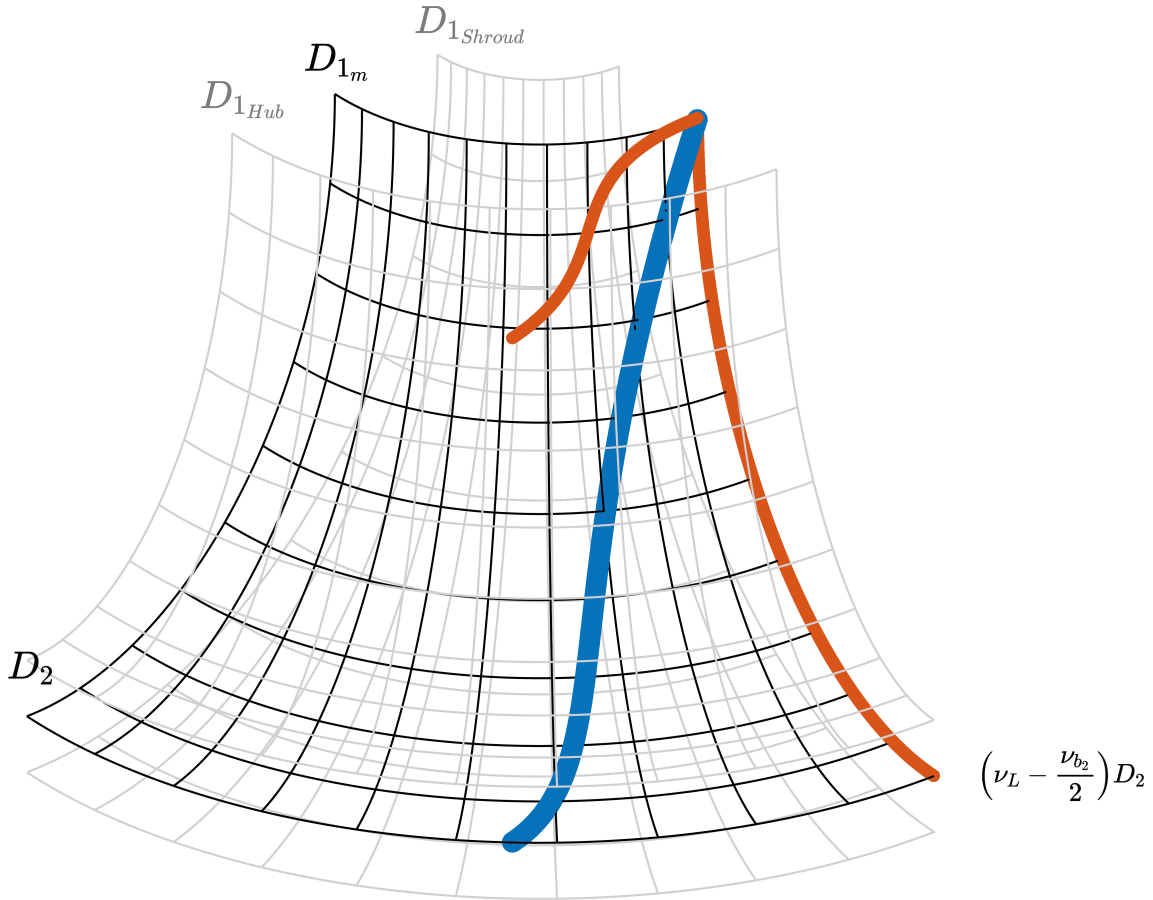
Figure 2: Bézier spline, quarter ellipse and combined chord.

In this research, all compressors are designed to use *air*. The value of the kinematic viscosity ν is taken from the tables provided in [10]. The kinematic viscosity is given as a function of pressure p and temperature t. It is interpolated to match the values, which are computed by the machine design: p_1, T_1.

The chord Reynold's number is thus completely defined. Many parameters influence its value. The relative velocity w_{1_m} is mainly affected by the machine's duty and size. However, the local definition of the impeller inlet area also influenced its value. The chord length is the other main influence on the Reynold's number's value. It is mostly driven by the impeller's outer diameter D_2, which is a global machine properties. Still, more parameters are included in its definition: the axial impeller extent ratio ν_L, the impeller inlet diameters $D_{1_{Hub}}$ and $D_{1_{Shroud}}$, the impeller exit width ratio ν_{b_2} as well as the circumferential and relative blade angle at the trailing edge θ_2 and β_2.

5   Conclusion

A method of computing the chord Reynold's number Re_c for radial turbocompressors without employing the actual impeller's *CAD* geometry was presented. A Bézier spline

and a quarter ellipse model the chord's coordinates. Both were combined to obtain the chord in Cartesian coordinates. They are defined using only the compressors principal dimensions, while neglecting the actual distribution of the blade angle and the actual shape of the meridional contour.

The model enables the computation and use of the chord Reynold's number in machine design process. Therefore, it may be computed after the machine design has been calculated to evaluate and compare the machine design. Additionally, it may be implemented in the machine design process when using an iterative process. This way, empirical models may be used to streamline the design process.

References

[1] Michael Casey. "The Effects of Reynolds Number on the Efficiency of Centrifugal Compressor Stages." In: *Journal of Engineering for Gas Turbines and Power* 107.2 (1985), pp. 541–548. ISSN: 0742-4795. DOI: 10.1115/1.3239767.

[2] Michael Casey and Chris Robinson. "A unified correction method for Reynolds number, size, and roughness effects on the performance of compressors." In: *Proceedings of the Institution of Mechanical Engineers, Part A: Journal of Power and Energy* 225.7 (2011), pp. 864–876. ISSN: 0957-6509. DOI: 10.1177/0957650911410161.

[3] Johann Friedrich Gülich. *Centrifugal Pumps.* Berlin, Heidelberg: Springer Berlin Heidelberg, 2008. ISBN: 978-3-540-73694-3. DOI: 10.1007/978-3-540-73695-0.

[4] Osborne Reynolds. "IV. On the dynamical theory of incompressible viscous fluids and the determination of the criterion." In: *Philosophical Transactions of the Royal Society of London. (A.)* 186 (1895), pp. 123–164. ISSN: 0264-3820. DOI: 10.1098/rsta.1895.0004.

[5] Werner Fister. *Fluidenergiemaschinen. Band 2: Auslegung, Gestaltung, Betriebsverhalten ausgewählter Verdichter- und Pumpenbauarten.* ger. Fister, Werner (author.) Berlin, Heidelberg: Springer Berlin Heidelberg, 1986. 606675 pp. ISBN: 978-3540154785. DOI: 10.1007/978-3-642-82524-8.

[6] S. L. Dixon and C. A. Hall. *Fluid mechanics and thermodynamics of turbomachinery.* eng. Seventh edition. Dixon, S. L. (VerfasserIn) Hall, C. A. (VerfasserIn). Amsterdam: Butterworth-Heinemann, 2014. 537 pp. ISBN: 9780124159549.

[7] Carl Pfleiderer and Hartwig Petermann. *Strömungsmaschinen.* ger. 7., unveränd. Aufl. Klassiker der Technik. Petermann, Hartwig (VerfasserIn). Berlin: Springer, 2005. 581 pp. ISBN: 978-3-540-26913-7.

[8] Michael Casey and Chris Robinson. *Radial Flow Turbocompressors.* en. Cambridge University Press, 2021. ISBN: 9781108416672.

[9] Ekbert Hering, Rolf Martin, and Martin Stohrer. *Taschenbuch der Mathematik und Physik.* Berlin, Heidelberg: Springer Berlin Heidelberg, 2017. ISBN: 978-3-662-53418-2. DOI: `10.1007/978-3-662-53419-9`.

[10] Peter Stephan et al., eds. *VDI-Wärmeatlas. Fachlicher Träger VDI-Gesellschaft Verfahrenstechnik und Chemieingenieurwesen.* ger. Living reference work, continuously updated edition. VDI Springer Reference. Stephan, Peter (HerausgeberIn) Kind, Matthias (HerausgeberIn) Schaber, Karlheinz (HerausgeberIn) Wetzel, Thomas (HerausgeberIn) Mewes, Dieter (HerausgeberIn) Kabelac, Stephan (HerausgeberIn) Stephan, Peter, (Herausgeber.) Mewes, Dieter, (Herausgeber.) Kabelac, Stephan, (Herausgeber.) Kind, Matthias, (Herausgeber.) Schaber, Karlheinz, (Herausgeber.) Wetzel, Thomas, (Herausgeber.) Berlin, Heidelberg: Springer Berlin Heidelberg, 2019. 1 online resource. ISBN: 9783662529911. DOI: `10.1007/978-3-662-52991-1`.